

# **Anodic Stripping Voltammetry with Graphite Felt Electrodes for the Trace Analysis of Silver: Supporting Information**

Trevor J. Davies

Department of Natural Sciences, University of Chester, Thornton Science Park, Pool Lane,  
Ince, Cheshire, UK, CH2 4NU.

To be submitted to The Analyst

Email: [t.davies@chester.ac.uk](mailto:t.davies@chester.ac.uk)

Tel.: +44 (0)1244 512297

## 1. Estimation of graphite felt physical properties

In previous work with the same felt (SGL GFD2.5) scanning electron microscopy was used to determine the diameter of the fibres within the carbon felt.<sup>1</sup> The fibres were found to have an average diameter of 8  $\mu\text{m}$  from a range of measurements.<sup>1</sup> The electrochemical surface area (or “smooth” surface area) of the felt can be estimated by approximating the felt as one smooth cylindrical carbon fibre of 8  $\mu\text{m}$  diameter. The mass of the felt electrode,  $m$ , can be used to determine the total volume of the carbon fibres,  $V_{\text{cf}}$ , via the simple density relationship:

$$V_{\text{cf}} = \frac{m}{\rho_{\text{cf}}} \quad (\text{S1})$$

where  $\rho_{\text{cf}}$  is the density of carbon fibres and is generally considered to be around 1.8  $\text{g cm}^{-3}$ .<sup>2,3</sup> The equivalent length of the single carbon fibre,  $L_{\text{cf}}$ , is then deduced using the equation for the volume of a cylinder:

$$\pi r^2 L_{\text{cf}} = V_{\text{cf}} \quad (\text{S2})$$

where  $r$  is the radius of the carbon fibre (4  $\mu\text{m}$  for the felt used in this investigation). The surface area of the fibre (and hence the whole electrode),  $A_{\text{cf}}$ , is then determined using:

$$A_{\text{cf}} = 2 \pi r L_{\text{cf}} \quad (\text{S3})$$

Combining equations S1, S2 and S3, it is possible to estimate the electrochemical surface area of the felt electrode by weighing the felt sample:

$$A_{\text{cf}} = \frac{2m}{r\rho_{\text{cf}}} \quad (\text{S4})$$

For example, felt sample “GF2” in Figure S3 (below) had a mass of 0.0211 g. Using equation S4 and the values for  $\rho_{\text{cf}}$  and  $r$  given above, this gives an estimated electrochemical surface area of 58.6  $\text{cm}^2$  for the 1 x 1 x 0.28 cm sample.

Once the mass of the felt sample is known, the porosity,  $\phi$ , of the felt electrode can be determined using Equation S5:

$$\phi = 1 - \frac{m}{V_{\text{tot}}\rho} \quad (\text{S5})$$

where  $V_{\text{tot}}$  is the volume of the sample, in this case 0.28  $\text{cm}^3$ . For example, in the case of felt sample “GF2” above, the porosity is 0.96 (or 96%). From the definition of porosity it follows the volume of the voids,  $V_{\text{void}}$ , is given by:

$$V_{\text{void}} = \phi V_{\text{tot}} \quad (\text{S6})$$

## 2. Silver Anodic Stripping Voltammetry in 0.1 M Nitric Acid

Figures S1 and S2 show results from experiments used to optimize the Ag deposition parameters with GF (graphite felt) electrodes in 0.1 M HNO<sub>3</sub>. Figure S1 illustrates the effect of deposition time and Figure S2 illustrates the effect of deposition potential. The platinum wire used to connect to the GF electrodes was found to limit the magnitude of the deposition potential. A deposition potential of -0.7 V resulted in a distorted stripping signal with a steeper baseline. Lower deposition potentials gave very poor signals at much higher currents due to the production of hydrogen at the platinum wire, which became trapped inside the GF. Given these results it was decided to use a deposition potential of -0.6 V vs. Hg/Hg<sub>2</sub>SO<sub>4</sub> for 90 s for the sensor development. Similar results were obtained for GF electrodes in the 0.1 M HNO<sub>3</sub> / 14 mM KCl system, and identical deposition conditions were used (-0.6 V vs. Hg/Hg<sub>2</sub>SO<sub>4</sub> for 90 s). Optimization of the deposition conditions for the PFC (pyrolytic formed carbon) and EPPG (edge plane pyrolytic carbon) followed a similar procedure with almost identical results to those in the literature (-0.8 V vs. Hg/Hg<sub>2</sub>SO<sub>4</sub> for 120 s in 0.1 M HNO<sub>3</sub> and -0.9 V vs. Hg/Hg<sub>2</sub>SO<sub>4</sub> for 120 s in 0.1 M HNO<sub>3</sub> / 14 mM KCl).<sup>7,8</sup>

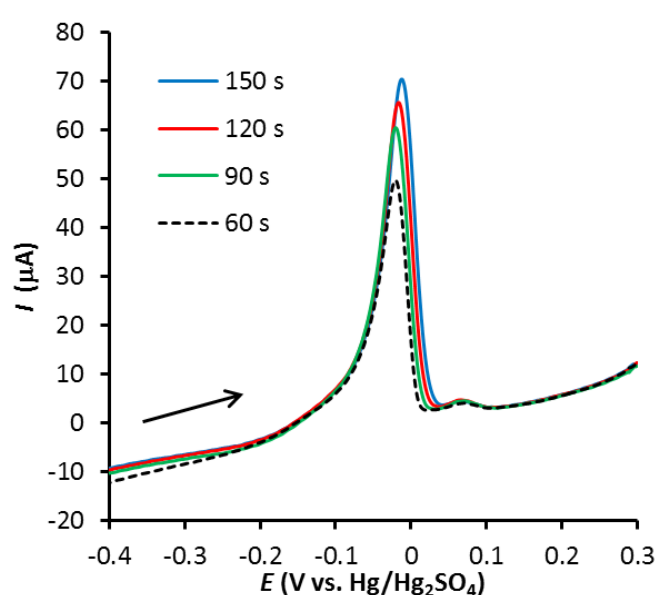


**Figure S1.** Linear sweep voltammograms ( $50 \text{ mV s}^{-1}$ ) for the anodic stripping of Ag in  $2.5 \mu\text{M AgNO}_3 / 0.1 \text{ M HNO}_3$  at a GF electrode with approximate surface area  $58 \text{ cm}^2$  and volume  $0.28 \text{ cm}^3$  (arrow indicates scan direction). The silver deposition step occurred at  $-0.5 \text{ V vs. Hg/Hg}_2\text{SO}_4$  for various times (60, 90, 120 and 150 s).

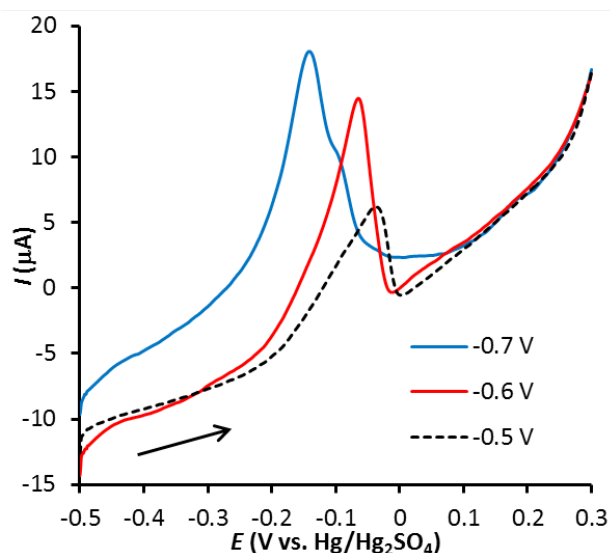


**Figure S2.** Linear sweep voltammograms ( $50 \text{ mV s}^{-1}$ ) for the anodic stripping of Ag in  $1 \mu\text{M AgNO}_3 / 0.1 \text{ M HNO}_3$  at a GF electrode with approximate surface area  $59 \text{ cm}^2$  and volume  $0.28 \text{ cm}^3$  (arrow indicates scan direction). Electrode preconditioned at  $0.2 \text{ V}$  for  $30 \text{ s}$  then Ag deposition at various potentials ( $-0.5$ ,  $-0.6$  and  $-0.7 \text{ V}$  vs.  $\text{Hg}/\text{Hg}_2\text{SO}_4$ ) for  $120 \text{ s}$ .

Figure S3 illustrates linear sweep stripping voltammograms ( $50 \text{ mV s}^{-1}$ ) from experiments performed with a GF electrode in  $0.1 \text{ M HNO}_3$  with increasing amounts of  $\text{Ag}^+$ . In this case the GF electrode was preconditioned at  $0.2 \text{ V}$  for  $10 \text{ s}$  and Ag deposition occurred at  $-0.6 \text{ V}$  for  $120 \text{ s}$ . On increasing the  $\text{Ag}^+$  concentration from  $0 \text{ M}$ , a silver signal is observed once  $[\text{Ag}^+]$  reaches  $10 \text{ nM}$ . This is slightly lower than the limit of detection evaluated in the main article (the latter obtained using a shorter Ag deposition time).

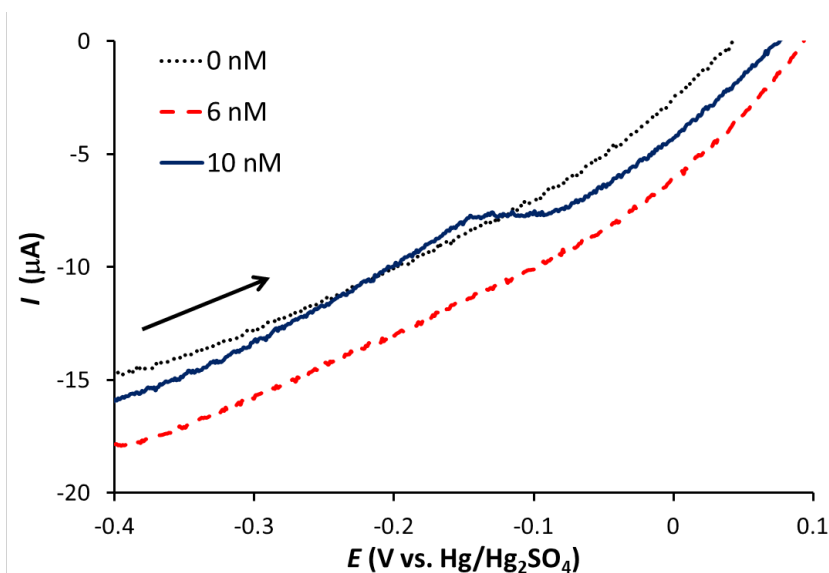


**Figure S3.** Linear sweep voltammograms ( $50 \text{ mV s}^{-1}$ ) for the anodic stripping of Ag in  $0.1 \text{ M HNO}_3$  at a GF electrode with approximate surface area  $60 \text{ cm}^2$  and volume  $0.28 \text{ cm}^3$  (arrow indicates scan direction). Electrode preconditioned at  $0.2 \text{ V}$  for  $10 \text{ s}$  then Ag deposition at  $-0.6 \text{ V}$  for  $120 \text{ s}$ .

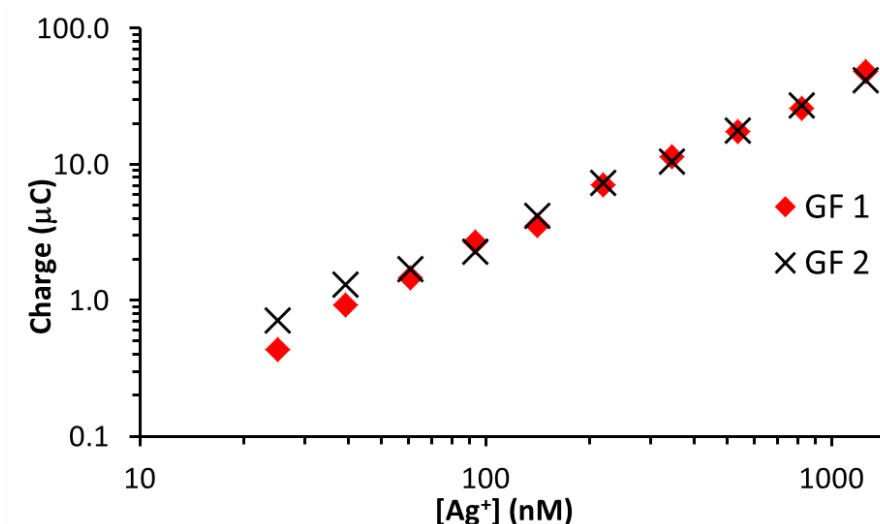


**Figure S4.** Stripping charge vs.  $\text{Ag}^+$  concentration for the linear sweep anodic stripping of Ag in 0.1 M  $\text{HNO}_3$  at  $50 \text{ mVs}^{-1}$  with two different GF electrodes in 0.1 M  $\text{HNO}_3$ . GF electrodes were preconditioned at 0.2 V for 10 s and Ag deposition occurred at -0.6 V for 90 s, followed by stripping. Approximate surface areas are  $55 \text{ cm}^2$  for GF 1 and  $59 \text{ cm}^2$  for GF2. Approximate volume for both electrodes is  $0.28 \text{ cm}^3$ .

Figure S4 illustrates plots of stripping peak charge vs.  $\text{Ag}^+$  concentration for the linear sweep stripping voltammograms ( $50 \text{ mV s}^{-1}$ ) obtained with two different GF electrodes in 0.1 M  $\text{HNO}_3$ . Both GF electrodes had dimensions  $1 \times 1 \times 0.28 \text{ cm}$ , with masses of 0.0198 g (GF1) and 0.0211 g (GF2). As observed, the results for the two electrodes are very similar, demonstrating the good repeatability attainable with these electrodes. A key factor to the good repeatability is the electrode wetting procedure, which ensures repeatable wetting of the interior surface of the GF electrodes.

Differential pulse voltammetry (DPV) was also used to generate stripping signals (after the same preconditioning and Ag deposition steps used for linear sweep experiments). Optimum DPV parameters were found using a  $2.5 \mu\text{M}$  solution of  $\text{AgNO}_3$  in 0.1 M  $\text{HNO}_3$ . These were 0.03 s modulation time; 0.1 s Interval time; 50 mV amplitude; 4 mV step potential for GF electrodes and 0.01 s modulation time; 0.1 s Interval time; 100 mV amplitude; 4 mV step potential for PFC and EPPG electrodes. The results for the GF and PFC electrodes are shown in Figure S5 (the EPPG results were very similar to those for PFC). In this case, linear sweep voltammetry provided better signals than DPV.

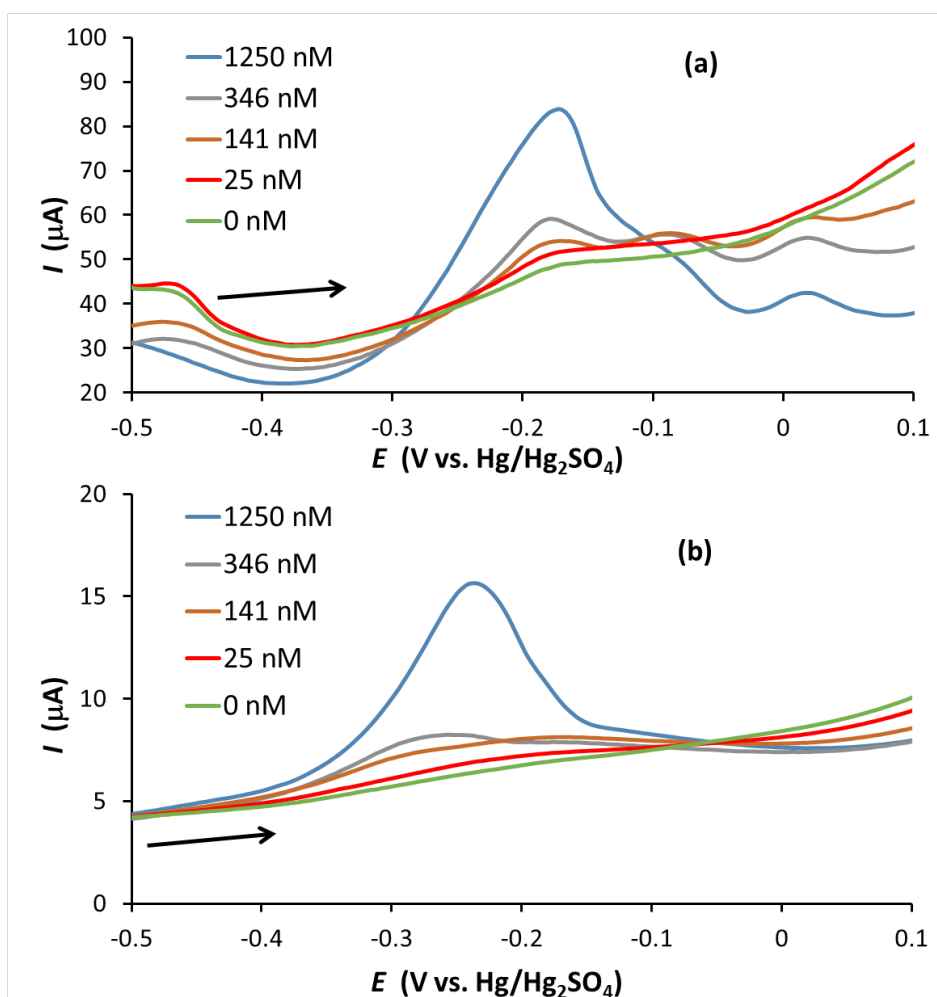


**Figure S5.** Differential pulse voltammograms for the anodic stripping of Ag in 0.1 M HNO<sub>3</sub> at a (a) GF electrode with approximate surface area 55 cm<sup>2</sup> and volume 0.28 cm<sup>3</sup> and (b) PFC electrode with surface area 0.07 cm<sup>2</sup>, where 0 nM < [Ag<sup>+</sup>] < 1250 nM (arrow indicates scan direction). GF DPV Parameters: 0.03 s modulation time; 0.1s interval time; 50 mV amplitude; 4mV step potential. PFC DPV Parameters: 0.01 s modulation time; 0.1s interval time; 100 mV amplitude; 4mV step potential. Electrode preconditioned at 0.2 V for 10 s followed by Ag deposition at -0.6V for 90 s (GF) or -0.8 V for 120 s.

### 3. Silver Anodic Stripping Voltammetry in 0.1 M Nitric Acid and 14 mM KCl

Figure S6 illustrates linear sweep voltammograms obtained with PFC and GF electrodes at different concentrations of Ag<sup>+</sup> in 0.1 M HNO<sub>3</sub> and 14 mM KCl. This system has previously been found to produce sharper stripping signals allowing a lower limit of detection.<sup>4,5</sup> The anodic stripping of Ag at 0.05 V s<sup>-1</sup> followed preconditioning at 0.2 V for 30 s (PFC) or 10 s (GF) and a deposition step of -0.9 V for 120 s (PFC) or -0.6 V for 90 s (GF). For the PFC electrode, an Ag signal was observed from 102 nM upwards (the EPPG results were similar). The corresponding concentration was 73 nM for the GF electrode, suggesting a slightly lower limit of detection than conventional carbon electrodes, but not as low as that achieved in the absence of KCl.

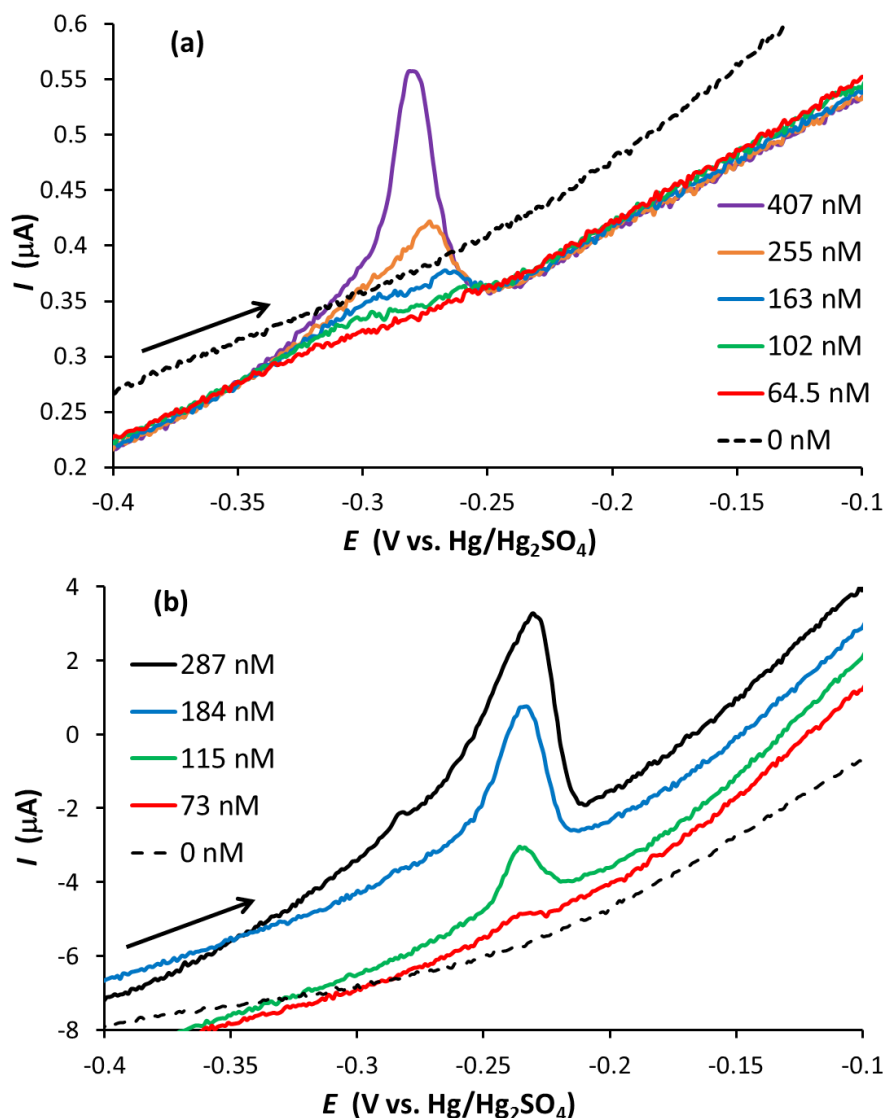


**Figure S6.** (a) Linear sweep voltammograms ( $50 \text{ mV s}^{-1}$ ) for the anodic stripping of Ag in 0.1 M  $\text{HNO}_3$  and 14 mM KCl with a (a) PFC electrode with surface area  $0.07 \text{ cm}^2$  and (b) GF electrode with approximate surface area  $53 \text{ cm}^2$  and volume  $0.28 \text{ cm}^3$  in a range of silver concentrations (arrow indicates scan direction). PFC Electrode preconditioned at 0.2 V for 30 s followed by Ag deposition at -0.9 V for 120s. GF Electrode preconditioned at 0.2 V for 10 s followed by Ag deposition at -0.6 V for 90s.

#### 4. Estimation of Pore Depletion

Using the model of Smith and co-workers,<sup>1</sup> a tubular pore of diameter  $d$  within a GF electrode can be approximated as a parallel plate electrode arrangement with the same surface area and plate separation of  $d$ . This can be further simplified to a plate electrode opposite a parallel insulating plate separated by a distance  $\frac{1}{2}d$ . This arrangement can be simulated in DigiElch using the finite diffusion option with an insulating boundary.<sup>6</sup> Accordingly, simulations were performed to determine the extent of  $\text{Ag}^+$  depletion with the pores of GF during the Ag deposition step. Finite diffusion chronoamperometry simulations were performed using DigiElch, with an electrode of  $1 \text{ cm}^2$  surface area opposite an insulating boundary and a redox species of diffusion coefficient  $1.55 \text{ cm}^2 \text{ s}^{-1}$  (representative of aqueous  $\text{Ag}^+$ ). A potential step was imposed on the electrode such that the redox species underwent rapid reduction at the electrode surface (i.e. zero concentration of  $\text{Ag}^+$  at the electrode surface). The concentration profile of the redox species was monitored and the time taken to achieve full depletion within the thin layer was determined. This was repeated

for a range of values of the electrode-insulator distance (“width of thin layer”). The results are shown in Figure S7. As observed, at 90 s thin layers of less than 240  $\mu\text{m}$  width are fully depleted. Using the approximation above, this corresponds to a pore of diameter 480  $\mu\text{m}$ . Therefore, the threshold pore diameter,  $d_{\text{limit}}$ , below which full depletion of the redox species within the pore occurs within 90 s is approximately 480  $\mu\text{m}$  for the  $\text{Ag}^+$  solutions studied.

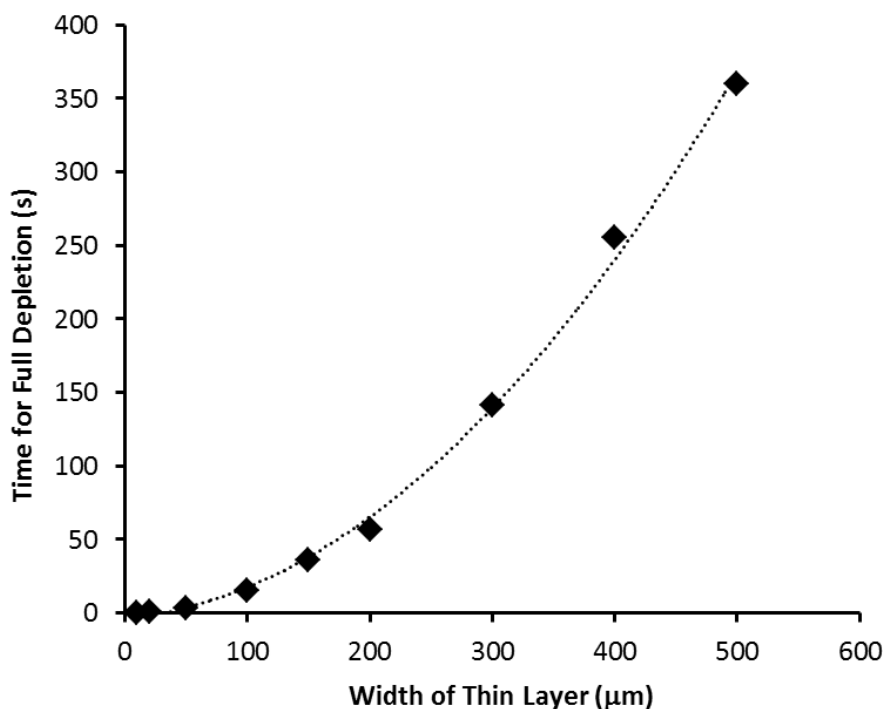


**Figure S7.** Depletion time vs. thin layer width obtained from DigiElch chronoamperometry finite diffusion simulations, representing the depletion of  $\text{Ag}^+$  within the GF pores during the silver deposition step.

## 5. References

- [1] R.E.G. Smith, T.J. Davies, N.B. Baynes, R.J. Nichols, *J. Electroanal. Chem.* 2015, **747**, 29.
- [2] B. Delanghe, S. Tellier, M. Astruc, *Electrochimica Acta*, 1990, **35**, 1369.
- [3] R.L. McCreery, in: A. J Bard (Ed.), *Electroanalytical Chemistry*, volume 17, Marcel Dekker, New York, 1990, 221.
- [4] F. Wantz, C. E. Banks, R. G. Compton, *Electroanalysis*, 2005, **17**, 655.
- [5] A. J. Saterlay, F. Marken, J. S. Foord, R. G. Compton, *Talanta*, 2000, **53**, 403.
- [6] <http://www.elchsoft.com/digielch/DigiElch7/Default.aspx>
- [7] Metrohm Application Bulletin No. 207/2 e.
- [8] F. Wantz, C. E. Banks, R. G. Compton, *Electroanalysis*, 2005, **17**, 655.